VERTICAL AXIS WIND TURBINE PERFORMANCE PREDICTION MODELS USING HIGH AND LOW FIDELITY ANALYSES

Franklyn Kanyako, Masdar Institute of Science and Technology, UAE; Isam Janajreh, Masdar Institute of Science and Technology, UAE

Abstract

Vertical axis wind turbines have potential advantages for small domestic applications, as they can be effectively used in urban areas, where wind is intermittently unsteady and turbulent. In this paper, the authors highlight the progress made in the development of aerodynamic models for predicting the performance of straight-bladed, fixed-pitch vertical axis wind turbine blade profiles. An improved low-fidelity blade element momentum algorithm using a hybrid database was built to investigate the solidity of the turbine by analyzing the effect of blade chord, radius, and number of blades at different tip speed ratios. This was followed by a 2D numerical investigation to compare the performance prediction capability of computational fluid dynamics (CFD) and mathematical models. Both high- and low-fidelity analyses showed minimum/negative performance at low tip speed ratios, indicating the general inability of the fixed-pitch vertical axis turbine to self-start. The CFD analysis, though computationally intensive, showed better performance than the analytical solution and also captured important flow features such as vortex shedding, among other detailed flow field features.

Introduction

The development of wind turbine technologies has allowed wind energy to perform a relevant step forward in local production of clean electric power inside the built environment. The present technical design relies exclusively on horizontal axis turbines and is not yet adequate to develop reliable wind energy converters, particularly for conditions corresponding to low wind speeds and/or urban areas. This has renewed interest in Vertical Axis Wind Turbines (VAWT) like the Darrieus turbine, which appear to be particularly promising for such conditions. These VAWTs turbines can be used to power remote or off-grid applications such as homes, farms, refuges, or beacons. Intermediate-sized wind power systems (100 kW to 250 kW) can power a village or a cluster of small enterprises and can be grid-connected or off-grid. They can also be coupled with diesel generators, batteries, and other distributed energy sources for remote use, where there is no access to the grid design. However, the disadvantages of VAWTs stem from the fact that there is cyclical variation in the angle of attack on the aerofoils as the rotor rotates. As a result, optimal loading cannot be sustained for all azimuthal angles, leading to inherently low aerodynamic efficiency compared to horizontal axis wind turbines (HAWT) [1]. The rotation of the turbine in 3D environments leads to several flow phenomena—such as dynamic stall, flow separation, and flow wake deformation—making the aerodynamic analysis and performance prediction of the Darrieus wind turbine very difficult. Currently, there are various computational models present, which have their own strengths and weaknesses, with the goal to accurately predict the performance of a wind turbine. Predicting wind turbine performance numerically offers a possibility to reduce the expensive and exhaustive wind tunnel and field experimental tests, the major benefit of which being that computational studies are more economical, versatile, and afford higher resolution than costly experiments.

Computational Models for VAWT

Despite the complexity of the aerodynamic behavior of the Darrieus VAWT, several mathematical models have been proposed for the performance prediction and design of the Darrieus VAWT. Based on a survey of aerodynamic models used for prediction of VAWT performance [1], [2], these models can be broadly classified into three categories, according to their increasing complexities: 1) momentum models, 2) vortex model, and 3) computational fluid dynamics (CFD).

The momentum model combines momentum theory with blade element theory [3]. It studies the behavior of the air flow on the blades and its forces. They can be further divided into single-stream tube, multiple-stream tube, and double -multiple stream tube models. In the single-stream tube model, first developed by Templin [4] for VAWTs, the turbine is placed inside a single-stream tube and its blades revolution is translated in an actuator disk. The effects of the stream tube outside are assumed negligible and the wind speed in the upstream and downstream sides of the turbine are assumed to be constant. This model suffers from performance accuracy prediction, due to the many assumptions and usually gives higher prediction values.

The multiple-stream tube model, developed by Strickland [5], is a variation of the single-stream tube model, where the single-stream tube is divided into several parallel adjacent stream tubes that are independent of each other and have their own undisrupted, wake and induced velocities. Several modifications/corrections have been incorporated into this model, where the drag forces, aerofoil geometry, curvature flow, etc., were added, while it provides relatively better accuracy than the single stream as it still lacks experimental validation. The double-multiple stream tube (DMS) model is a variation of the multiple-stream tube model, where the actuator disc is divided into two half cycles in tandem, representing the upstream and downstream sides of the rotor. This model was presented by Paraschivoiu [6].

The vortex models are basically potential flow models based on the calculation of the velocity field about the turbine through the influence of vorticity in the wake of the blades. The turbine blades are represented by bound or lifting-line vortices whose strengths are determined using airfoil coefficient datasets and calculated relative flow velocity and angle of attack. Larsen [7] first introduced the idea of a vortex model for a single-blade element of a VAWT. He used the vortex model for the performance prediction of a cyclogiro windmill. The model is a two-dimensional one but, if the vortex trailing from the rotor blade tips is considered, it may be said that it is not strictly two-dimensional. However, in his model, angle of attack is assumed to be small; as a result, the stall effect is neglected. Strickland et al. [8] presented an extension of the vortex model, which is a three-dimensional one in which the aerodynamic stall is incorporated into the model. They presented the experimental results for a series of two-dimensional rotor configurations. Their calculated values showed good correlation with the experimental results for the instantaneous blade forces and the near wake flow behind the rotor. Strickland et al. also made improvements on the prior vortex model. The latest model is termed as the dynamic vortex model since, in this model, the dynamic effects are included. The improvements over the prior model are that it includes the dynamic stall effect, pitching circulation, and added mass effect. The main disadvantage of the vortex model is that it takes too much computation time. Furthermore, this model still relies on significant simplifications (e.g., potential flow is assumed in the wake and the effect of viscosity in the blade aerodynamics is included through empirical force coefficients) [9].

Computational fluid dynamics (CFD) is widely employed for VAWT performance analysis. It solves the Reynolds Averaged Navier-Stokes equation or the more advanced and costly Direct Numerical Simulation (DNS), Large Eddy Simulation (LES), and Detached Eddy Simulation (DES). Dobrev and Massouh [10] conducted high-fidelity simulations to explore the possibility of using 3D Navier-Stokes solver Detached Eddy Simulation solver (DES)/ /k-w model and Particle Image Velocimetry (PIV) for experimental validation. The comparison of wake and shedding vorticity with experiments shows that the 3D/k-w modeling gives results quite similar to phase-averaged velocity. The power coefficient measured was very close to the experimental results, confirming the capability of the DES model to accurately capture the turbulent detached flow. Mohamed [11] carried out an aerodynamic investigation for 20 different airfoils using a 2D, unsteady Reynolds averaged Navier Stokes (RANS) simulation. He found the S-1046 profile for the H-Darrieus rotor very promising for wind energy generation, in particular in urban areas compared to symmetric airfoils. Many other studies have been done using RANS [12-14]; however, CFD is computationally intensive, as the aerodynamic performance of the turbine is a function of their instantaneous forces and moment coefficient. The objective of this current study was to investigate some of the most significant parameters that affect turbine performance such as turbine solidity, number of blades, airfoil selection, and turbine aspect ratio (H/D). In this paper, the authors focused on understanding the importance of these factors, specifically the first three to find the best configuration for the H-Darrieus turbines. This investigation was carried out by using a double-multiple stream model with a hybrid database of lift and drag coefficient prediction methodology from −180 °C to 180 °C, developed by Castelli et al. [15]. The result was compared with numerical simulations using the unsteady Reynolds averaged Navier stokes solver.

Aerodynamics Analysis of H-Darrieus VAWT

DMST Model: For the low-fidelity analysis, the DMST developed by Paraschivoiu [6] was adapted to a H-Darrieus based on the following assumptions: a) Unlike for the Troposkien/egg-shaped Darrieus turbine used by Paraschivoiu, it was assumed that no vertical variation of the induced velocity as straight vertical blade is subjected to the same flow velocity along its length—therefore, the angle δ that lies between the normal element to the blade element and horizontal XY plane is equated to zero ($\delta = 0$); b) It was assumed to be a fixed-pitch VAWT—therefore, using a symmetric airfoil section, the chord line is tangent to the circle of rotation (or blade flight path) and $a_o = 0$. Illustration of the straight 4-bladed Darrieus type VAWT is shown in Figure 1(a) and the aerodynamic characteristics are depicted in Figure 1(b). The relative velocity component, V_R, can be obtained from the cordial velocity and normal velocity components, as given by Equation (1):

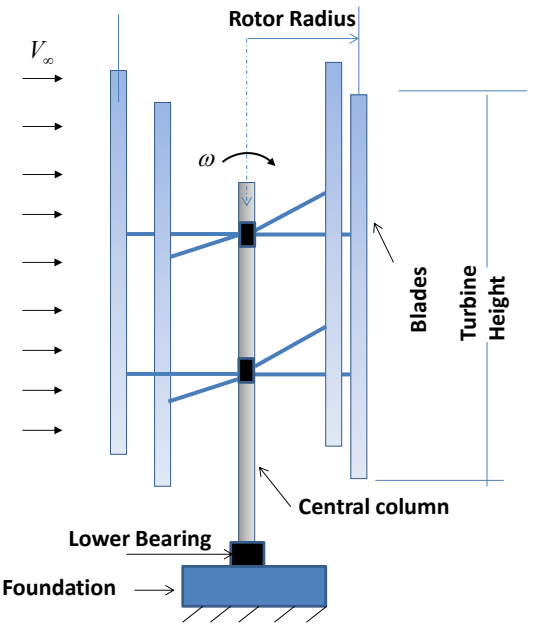

(a) Schematic of the Straight 4-bladed Darrieus Turbine

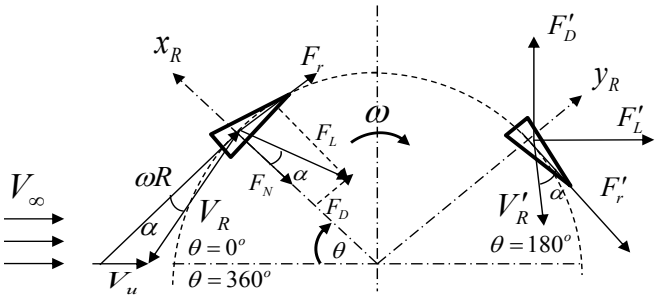

(b) Flow Within the Straight-bladed Darrieus Rotor

Figure 1. Illustration of the Flow Velocities of the Straight-bladed Darrieus Rotor

$$V_R = \sqrt{V_u^2[(x - \sin\theta)^2 + \cos^2\theta])} \tag{1}$$

where, V_u is the induced velocity, defined as the axial flow velocity through the rotor; θ is the azimuth angle; and, x is the local tip speed ratio (TSR), which is defined according to Equation (2):

$$x = \frac{\omega R}{V_u} \tag{2}$$

where, ω is the turbine's angular speed and R is the rotor radius. The fraction of the frontal swept area of the wind turbine covered by the blades represents the solidity, defined in Equation (3):

$$\sigma = \frac{NC}{R} \tag{3}$$

where, N is the number of blades; c is the chord length of the blades; and, R is the radius of the rotor. From the geometry in Figure 1, the expression for the local angle of attack may be derived by Equation (4):

$$\alpha = \sin^{-1}[\frac{\cos\theta}{\sqrt{(x - \sin\theta)^2 + \cos^2\theta}}] \tag{4}$$

The normal and tangential force coefficients are expressed by Equations (5) and (6):

$$C_n = C_L \cos\alpha + C_D \sin\alpha \tag{5}$$

$$C_t = C_L \sin\alpha + C_D \cos\alpha \tag{6}$$

where, C_L is the lift coefficient and C_D is the drag coefficient for angle of attack α. Then the normal and tangential forces for a single blade at a single azimuthal location can be written according to Equations (7) and (8):

$$F_N = \tfrac{1}{2}\rho V_R^2(h_C)C_n \tag{7}$$

$$F_T = \tfrac{1}{2}\rho V_R^2(h_C)C_t \tag{8}$$

where, h is the blade height and c is the blade chord length. Referring to Figure 1, the force of the wind on the turbine, which is experienced by one blade element in the direction of the air flow, is denoted as the instantaneous thrust force, according to Equation (9):

$$T_i = \tfrac{1}{2}\rho V_R^2(h_C)(C_n \sin\theta - C_t \cos\theta) \tag{9}$$

This is because the tangential force component creates the rotation of the wind turbine and generates the torque necessary to produce electricity. The instantaneous torque or the torque by a single blade at a single azimuthal location is described by Equation (10):

$$Q_i = F_T R \tag{10}$$

Substituting Equation (8) into Equation (10) yields Equation (11):

$$Q_i = \tfrac{1}{2}\rho V_R^2(h_C)C_t R \tag{11}$$

Figure 2 shows a diagram of the DMS model [16]. The actuator disc is divided into two with each having its own induced velocity. The induced velocity decreases along the axial stream tube direction, so the induced velocity in the upstream, V_{aui}, is less than the undisrupted wind speed, $V_{\infty i}$, which arrives to the stream tube. Between the upstream and the downstream there is an equilibrium induced velocity, V_{ei}, that is less than the V_{aui}.

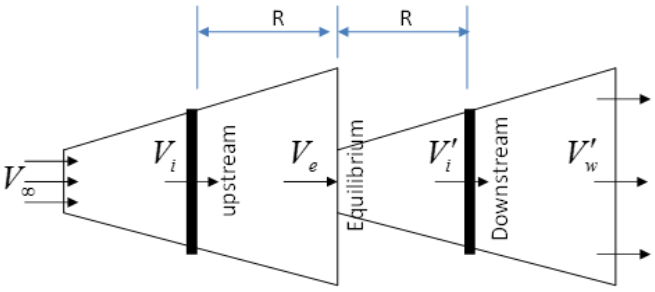

Figure 2. 2D Schematic of the DMST Model

The induced velocity in the downstream, V_{ad}, is less than V_{ei}. So Equation (12) yields the induced velocity in the upstream, V_{aui}:

$$V_{au} = V_{\infty i} K_{us} \tag{12}$$

where, K_{us} is the interference factor for the upstream, which is less than one and is given by Equation (13):

$$K_{us} = \frac{V_{au}}{V_{\infty i}} \tag{13}$$

The induced velocity in the midstream, V_e, is influenced by the wake velocity of the upstream, which is given by Equation (14):

$$V_e = V_{\infty i}(2\frac{V_{au}}{V_{\infty i}} - 1) = V_{\infty i}(2K_{us} - 1) \tag{14}$$

The induced velocity in the downstream, V_{ad}, is given by Equation (15):

$$V_{ad} = K_{ds} V_e = K_{ds}(2K_{us} - 1)V_{\infty i} \tag{15}$$

where, K_{ds} is the interference factor for the downstream and is given by Equation (16):

$$K_{ds} = \frac{V_{ad}}{V_e} \tag{16}$$

As can be seen, the aerodynamic behavior of the blades on the upstream side of the wind turbine will influence the induced velocity on the blades in the mid- and downstream regions. The undisrupted wind velocity, $V_{\infty i}$, is defined by the wind velocity profile and typically increases along the wind turbine height, according to a given local atmospheric boundary layer velocity profile. By applying the DMS model with the VAWT performance equations presented previously, it is possible to predict the turbine performance. The torque and power coefficients are found by integrating the aerodynamic behaviors of the various stream tubes. These iterative procedures, which are used in the DMST analysis, are illustrated in Figure 3. For the entire process, 36 stream tubes were used; and, evaluating the wind conditions at blade positions at five-degree increments, no significant difference was observed with an increase in the number of stream tubes. The induction factors a_u and a_d were calculated for the upstream and mid- and downstream tubes of the turbine, respectively.

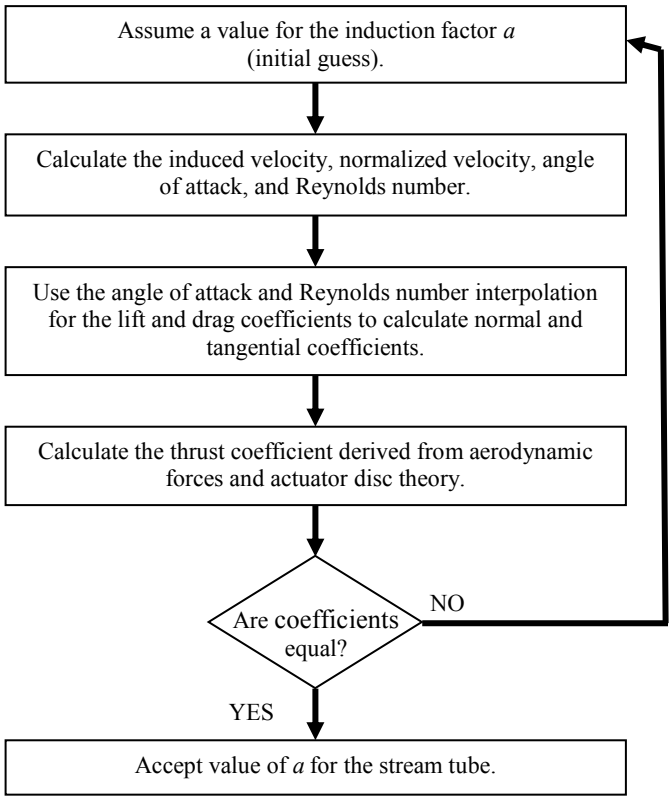

Figure 3. Iterative Procedure for Calculating the Flow Velocity in the DMST Model

CFD Model: The 2D wind turbine model was created using Gambit meshing software. The mesh and boundary conditions are shown in Figure 4, where the interior domain containing the wind turbine blades was considered as the moving mesh, while the outer domain was stationary. An unstructured grid was chosen for the moving and structured grid for the stationary domain. An interface was set between the interior sliding and outer stationary domain. The mesh on both sides of the interface had approximately the same characteristic cell size rendering the simulation more accurate and having faster convergence. The interior sliding domain rotated with a prescribed rotational velocity, ω. The inlet boundary was placed 5D upstream and the outlet placed at 20D downstream. The domain around the airfoil had to be wide enough to allow the vorticity and dynamic stall to fully develop. For both static and sliding models, the inlet boundary condition was velocity inlet. The upper and lower boundaries were assumed to be symmetrical, meaning

a zero normal gradient of pressure and velocity. The exit boundary was set as the pressure outlet in which the gauge pressure was set to zero gauge or atmospheric.

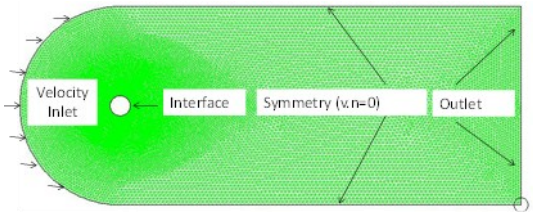

(a) The Fixed Domain of the Turbine

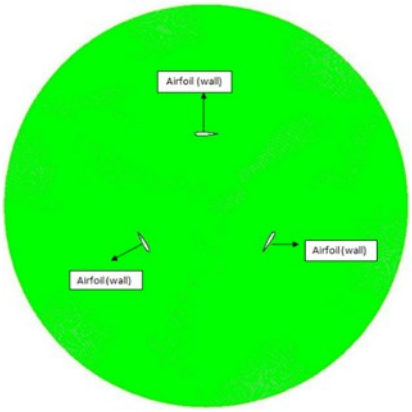

(b) The Rotating Domain of the Turbine Hub

Figure 4. Domain and Boundary Conditions for the 3-bladed VAWT

The boundary layer was placed on the blade profile, as shown in Figure 5, in order to capture the steep flow gradient at the airfoil surface and accurately determine lift, drag, and the separation of the flow from the blade surface. The average y+, which is the height of the first wall-adjacent cells inside the viscous sub-layer of the boundary layer, was set to 2E-5C, which corresponded to $y+ \leq 1$.

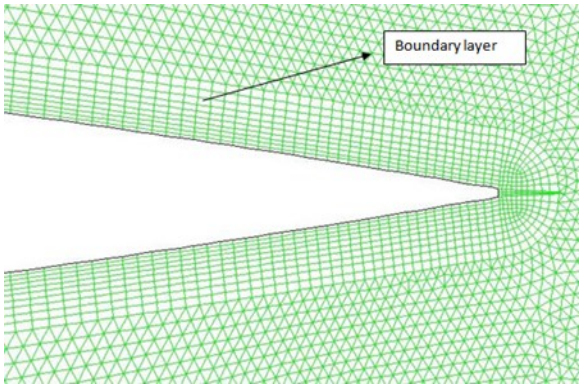

Figure 5. Boundary at the Trailing-edge of the Airfoil

For the simulation, Ansys Fluent was employed with a pressure-based segregated solver under the pressure correction SIMPLE algorithm, which accounted for the pressure-velocity coupling. A second-order spacila discretization scheme for the pressure derivative was used along with a second-order upwind discretization scheme for the advective velocity derivative and diffusive turbulent viscosity terms. A cell-based approach was used for the convective and diffusive gradients. A second-order implicit time integration was used for the temporal discretization at a minimum convergence criteria of 1e-07. A relatively small time step was used (ensuring algorithm stability) to properly model the transient phenomena. An SST-k-ω turbulence model was deployed as a conjugate solution of the two transport equations for k and ω for the evaluation of the eddy viscosity [17].

Results and Discussion

Figure 6 shows the coefficient of performance, C_p, comparison between the qualitative accuracy of the algorithm compared with the reference turbine. The C_p was evaluated from the fraction of the captured turbine power to the total available incoming wind power. A good approximation of the turbine performance up to the TSR value of five was observed, along with a slight over-estimation beyond that value. It should be noted that the algorithm took into account a varying interference factor as a function of the azimuth angle, but did not consider the vertical variation of the free-stream velocity. This explains the difference between the two results.

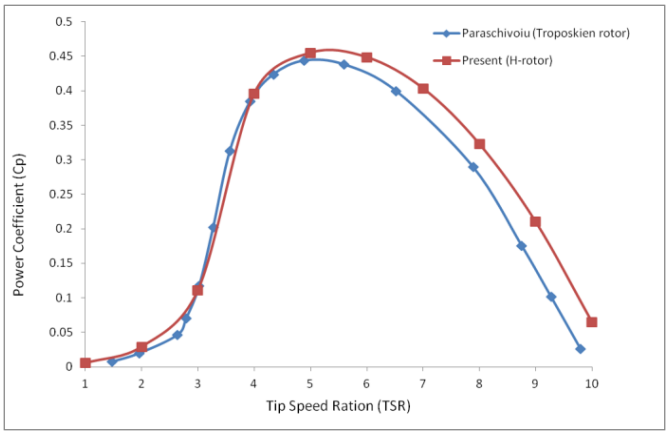

Figure 6. Comparison between the Current DMST Results and those found by Paraschivoiu et al. [17]

Figure 7 shows the C_p comparison between the CFD and DMST models. The C_p from the CFD analysis was found from the data file is reported here containing the dimensionless moment coefficient, C_m, per unit length. The torque and

power coefficients were calculated using Equations (17) and (18):

$$C_T = \frac{T}{\frac{1}{2}\rho U^2 AR} \tag{17}$$

$$C_p = \frac{T\omega}{\frac{1}{2}\rho U^3 A} \tag{18}$$

where, A and R are the area of the turbine and the radius, respectively; and, C_T and C_p are the torque and power coefficients.

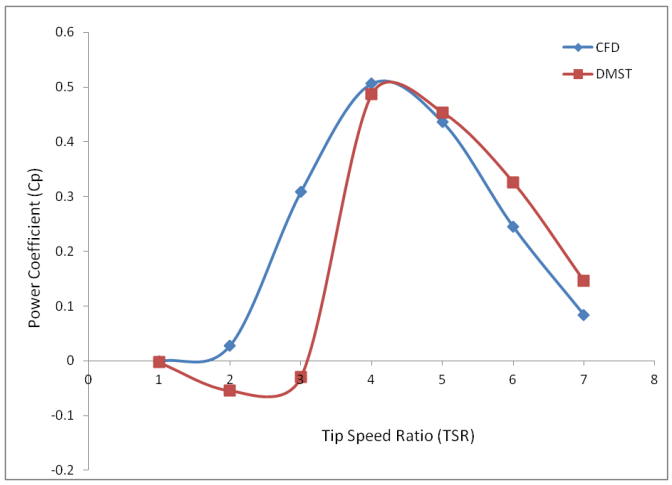

Figure 7. Power Coefficient Results for the DMST and CFD Models

As can be seen, both CFD and DMST model C_p curves show minimum torque for lower tip speed ratios. The DMST model underestimates the C_p value at lower tip speed ratios but predicted higher C_p values at higher tip speed ratios agree with results obtained by Salim and Cheah [17].

Effect of Blade profile: Darrieus VAWT has a positive angle of attack α at the front side of the rotor and a negative angle α at the back side, one has to use symmetrical airfoils. Three symmetric airfoils NACA 0015, NACA 0018, NACA 0021 which are frequently used for Darrieus VAWT are examined in this study. These airfoils have lower maximum lift coefficients if they are compared to asymmetrical airfoils of the same thickness. To realize a certain lift one must therefore use a larger chord.

From Figure 8, it can be seen that the self-starting behavior was improved with thicker airfoils (NACA 0021). The maximum efficiency of NACA 0021 is around 0.4657 at a TSR of 4; however, beyond TSR 4, the performance of the thicker blade becomes a disadvantage, as far as efficiency is concerned. It can also be observed that the results of NACA 0015 and NACA 0018 are close to each other, but the NACA 0018 has better starting performance, due to its thicker section.

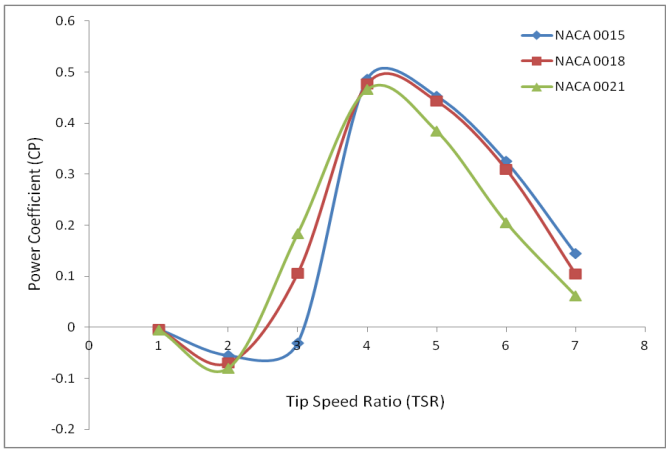

Figure 8. Power Coefficient for the Three Airfoils

Effect of number of blades: Figure 9 shows the effect of number of blades on C_p as a function of the tip speed ratio. As can be observed, the peak of C_p decreases as the number of blades increases. It can be said that a larger number of blades yields the maximum C_p for lower tip speed ratios, but yet are not as efficient compared to 3-bladed turbines. It can also be said that a larger number of blades improves starting performance of the turbine. For the 2-bladed turbines, though, it generates more power at higher tip speed ratios. Practically, then, the high rotational speed produces excessive vibration and, consequently, more noise and is not an optimal solution for urban installation. VAWTs with larger numbers of blades achieve maximum power at TSR; however, more blades will eventually decrease C_p.

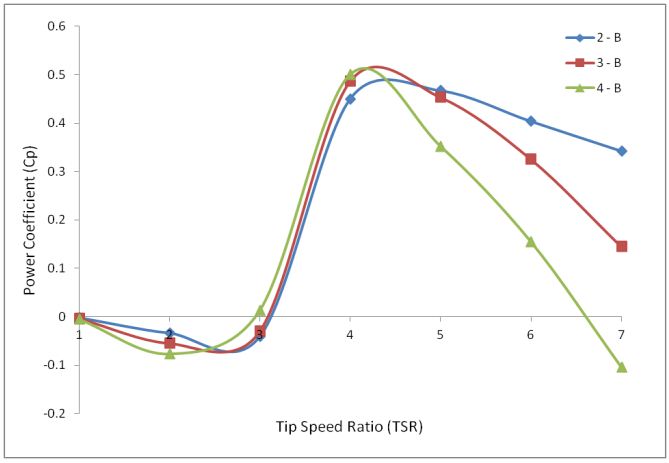

Figure 9. Power Coefficient as a Function of TSR for 2-, 3-, and 4-bladed Rotors

Figure 10 shows the evolution of instantaneous torque coefficient of the 2-bladed, 3-bladed, and 4-bladed turbines at a TSR of 3. It can be seen that, as the number of blades increases, the torque coefficient decreases. In a complete 360° rotation of the turbine, the number of periods becomes higher, as the number of blades increases, thereby creating a blocking effect and hindering air flow through the turbine. From the CFD analysis, the contour of vorticity, as shown in Figure 11, can be observed for 2- and 4-bladed turbines. This explains the decrease in the peak of the torque coefficient and power coefficient as the number of blades increases. It should be noted that this analysis was based on a 2D model, which is better suited to a straight-bladed turbine. Curved or twisted turbine blades mandate 3D treatment or a 2D piecewise layer-by-layer approach to account for the change in radius and angle of attack. Nevertheless, the 2D model captures the essence of the flow behavior and the trend, and considers a valuable conceptual design tool by avoiding the intensive computational demand and lead time of 3D preprocessing.

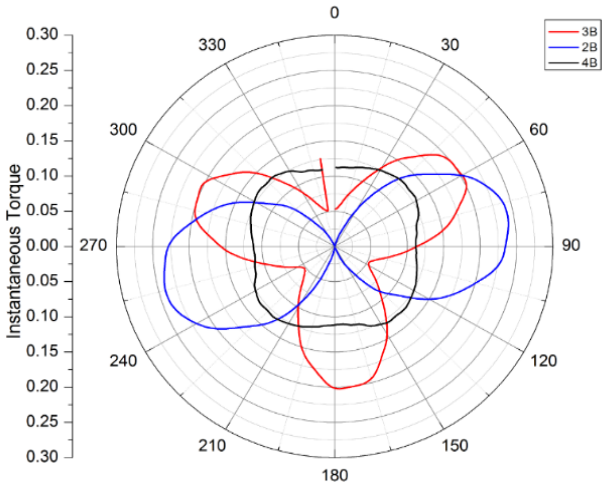

Figure 10. Instantaneous Torque Coefficient at TSR 3 for 2-, 3-, and 4-bladed Rotors

Conclusions

A low-fidelity analysis tool based on a double-multiple stream model was built using an extended airfoil database. It was validated using existing literature and a high fidelity numerical simulation based on Unsteady Reynolds Averaged Navier-Stoke equation. The results showed that the double-multiple stream tube (DMST) model was not suitable for high-solidity turbines and most suitable for low-solidity wind turbines. The disadvantage is that low-solidity turbines are not very applicable for built-in environments, due to its large radius, the anticipated high rotational speed, and associated noise. When the C_p values obtained from DMST and CFD analyses were compared, they showed that negative and/or minimum C_p and torque values are generated at lower tip speed ratios, which implies that NACA 0015, NACA 0018, and NACA 0021 airfoils are not self-starting. Nevertheless, NACA 0021 was shown to have better starting performance than the other two airfoils, due to its thicker section. CFD results were found to be more accurate and the flow physics like vorticity could be easily visualized. One major advantage of a low-fidelity analysis is that it can be used to determine an appropriate parameter for turbine performance before performing timely and expensive computations and experiments.

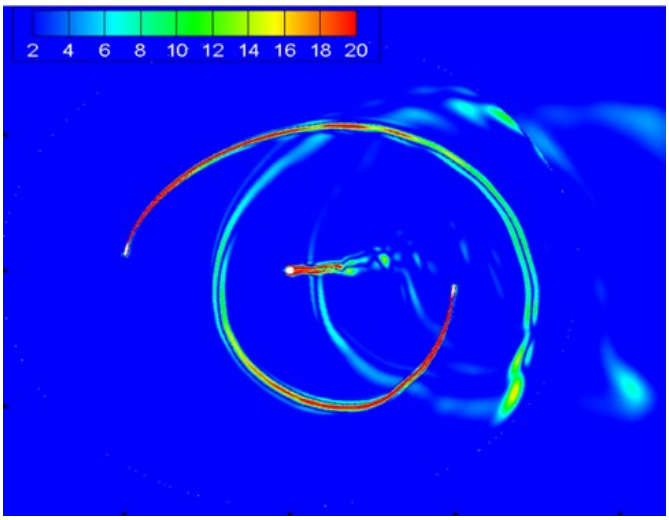

(a) Two-bladed Turbine Wake

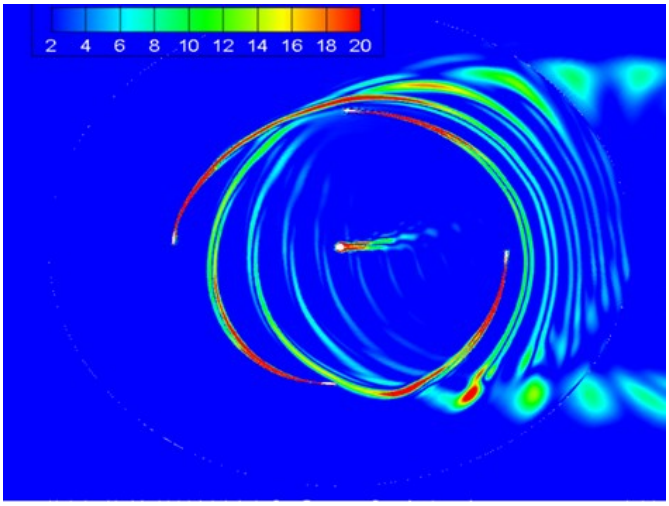

(b) Four-bladed Turbine Wake

Figure 11. Vorticity Contours of 2- and 4-bladed Rotating Turbines

References

[1] Bhutta, M. M., Hayat, N., Farooq, A. U., Ali, Z., Jamil, S. R., & Hussain, Z. (2012). Vertical Axis Wind Turbine – A Review of Various Configurations and Design Techniques. *Renewable and Sustainable Energy Reviews, 16*(4), 1926–1939.

[2] Islam, M., Ting, D., & Fartaj, A. (2008). Aerodynamic Models for Darrieus-type Straight-bladed Vertical Axis Wind Turbines. *Renewable and Sustainable Energy Reviews, 12*(4), 1087–1109.

[3] Paraschivoiu, I. (2002). Chapter 6: Double Actuator Disk Theory. In S. Schettini (Ed.), *Wind Turbine Design: With Emphasis on Darrieus Concept* (1st ed.), (pp. 147-259). Montreal, Canada: Presses Internationales Polytechnique.

[4] Templin, R. (1974). *Aerodynamic Performance Theory for the NRC Vertical-Axis Wind Turbine.* United States.

[5] Strickland, J. (1975). *The Darrieus Turbine: A Performance Prediction Model Using Multiple Streamtubes.* Albuquerque.

[6] Paraschivoiu, I. (1981). Double-Multiple Streamtube Model for Darrieus in Turbines. *NASA Lewis Research Center Wind Turbine Dynamics,* 19-25.

[7] Larsen, H. (1975). Summary of a Vortex Theory for the Cyclogyro. *Proceeding of the Second US National Conferences on Wind Engineering Research*, (pp. 1-3). Colorado.

[8] Strickland, J., Webster, B., & Nguyen, T. (1979). A Vortex Model of the Darrieus Turbine: An Analytical and Experimental Study. *Journal of Fluids Engineering,* (5), 101-500.

[9] Pawsey, N. (2002). *Development and Evaluation of Passive Variable-Pitch Vertical Axis Wind Turbine.* The University of New South Wales, Mechanical and Manufacturing Engineering.

[10] Dobrev, I., & Massouh, F. (2012). Exploring the Flow around a Savonius Wind Turbine. *International Symposium on Applications of Laser Techniques to Fluid Mechanics, 16*, 9-12.

[11] Mohamed, M. (2012). Performance Investigation of H-rotor Darrieus Turbine with New Airfoil Shapes. *Energy, 47*(1), 522–530.

[12] Howell, R., Qin, N., Edwards, J., & Durrani, N. (2010). Wind Tunnel and Numerical Study of a Small Vertical Axis Wind Turbine. *Renewable Energy, 35*(2), 412–422.

[13] Janajreh, I., Talab, I., & Macpherson, J. (2010). Numerical Simulation of Tower Rotor Interaction for Downwind Wind Turbine. *Modelling and Simulation in Engineering, 2010*, 1-11.

[14] Yao, Z. Q., & Yang, C. L. (2013). Numerical Simulation of Unsteady Flow for Variable-Pitch Vertical Axis Wind Turbine. *Applied Mechanics and Materials, 291-294*, 490-495.

[15] Castelli, M. R., Englaro, A., & Benini , E. (2014). A Proposal for a New Xfoil-Based Hybrid Extended Polar for Wind Turbine Applications. *ASME Journal of Solar Energy Engineering*.

[16] Paraschivoiu, I., Trifu, O., & Saeed, F. (2009). H-Darrieus Wind Turbine with Blade Pitch Control. *International Journal of Rotating Machinery, 2009*, 1 -7.

[17] Salim, S. M., & Cheah, S. C. (2009). Wall y+ Strategy for Dealing with Wall-bounded Turbulent Flows. *Proceedings of the International MultiConference of Engineers and Computer Scientists*, (pp. 2). Hong Kong.

Biographies

FRANKLYN KANYAKO is currently a Ph.D. candidate at Masdar Institute in Abu Dhabi, UAE. He is well-versed in wind turbine performance and analysis. His M.S. thesis work was on the development of low- and high-fidelity models for vertical wind turbines. Mr. Franklyn Kanyako may be reached fkanyako@masdar.ac.ae

ISAM JANAJREH is currently an Associate Mechanical Engineering Professor and the director of the wind and waste to energy lab at the Masdar Institute. He is an internationally recognized expert in the area of multiphysics flow, wind energy, and waste to energy, particularly in the feedstock characterization thermochemical pathways, including gasification and pyrolysis. He has authored more than 80 publications on the subject and appeared in over 80 conferences. Dr. Janajreh may be reached at ijanajreh@masdar.ac.ae